

PREPARED FOR SUBMISSION TO JINST

N<sup>TH</sup> WORKSHOP ON X

WHEN

WHERE

## A low-energy sensitive compact gamma-ray detector based on $LaBr_3$ and SiPM for GECAM

---

P Lv,<sup>a,b</sup> S.L Xiong,<sup>b</sup> X.L Sun,<sup>a,b,1</sup> J.G Lv,<sup>a,b</sup> Y.G Li<sup>b</sup>

<sup>a</sup>State Key Laboratory of Particle Detection and Electronics,  
Beijing 100049, China

<sup>b</sup>Institute of High Energy Physics, Chinese Academy of Sciences,  
Beijing 100049, China

E-mail: [sunxl@ihep.ac.cn](mailto:sunxl@ihep.ac.cn)

**ABSTRACT:** The Gravitational wave high-energy Electromagnetic Counterpart All-sky Monitor (GECAM) project is the planned Chinese space telescope for detecting the X and gamma-ray counterpart. It consists of two micro-satellites in low earth orbit with the advantages of instantaneous full-sky coverage, low energy threshold down to 6 keV and can be achieved within a short period and small budget. Due to the limitation of size, weight and power consumption of micro-satellites, silicon photomultipliers (SiPMs) are used to replace the photomultiplier tubes (PMTs) to assemble a novel gamma-ray detector. A prototype of a SiPM array with  $LaBr_3$  crystal is built and tested, and it shows a high detection efficiency (70% at 5.9 keV) and an excellent uniformity. The low-energy X-ray of 5.9 keV can be detected by a simply readout circuit, and the energy resolution is 6.5% (FWHM) at 662 keV. The design and performance of the detector are discussed in detail in this paper.

**KEYWORDS:** electromagnetic counterpart, gamma-ray detector,  $LaBr_3$  crystal, SiPM, low threshold, energy resolution

---

<sup>1</sup>Corresponding author.

---

## Contents

<b>1</b>	<b>Introduction</b>	<b>1</b>
<b>2</b>	<b>The GRD Structure</b>	<b>2</b>
<b>3</b>	<b>The Test System</b>	<b>2</b>
<b>4</b>	<b>The Detector Performance</b>	<b>3</b>
4.1	The low-energy performance	3
4.2	Energy Resolution	4
4.3	linearity	5
4.4	Uniformity	6
<b>5</b>	<b>Discussion and Summary</b>	<b>7</b>

---

## 1 Introduction

First gravitational wave event GW150914 [1–3] and double neutron star merger event GW170817 [4], heralded the new era of gravitational wave multi-messenger astronomy. The energy zone from keV to MeV is an important window for electromagnetic counterpart research. The two micro-satellites of GECAM, which are in the same low earth orbit with opposite orbital phase for full-sky coverage, are planned to launch in 2020. Each satellite consists of 25 gamma-ray detectors (GRD) and 8 charged-particle detectors (CPD). As the main instrument, GRD is used to monitor electromagnetic counterparts of gravitational wave events from 6 keV to 2 MeV.

PMT has a large volume and a high operating voltage, which make it inappropriate for micro-satellites. SiPM, a novel silicon-based photodetector, maintains attractive capabilities such as a large dynamic range, single-photon sensitivity, high photon detection efficiency, insusceptibility to magnetic fields and low bias [5]. However, the high thermal-noise [6] of large area SiPMs is an obstacle to detect low-energy rays especially below 10 keV, because the capacitance increases as the area of SiPM rises prolongs the decay time and decreases the amplitude for each signal. So the light yield of crystal is a critical parameter to make low-energy rays can be detected. The  $LaBr_3$  crystal is a good candidate because of its fast decay time (16 ns) and high light yield (>60,000 photons/MeV) [7–9], both result in a very good energy resolution and linearity. A prototype is designed with a  $LaBr_3$  crystal (76.2 mm in diameter) and a SiPM array ( $50.44 \times 50.44 \text{ mm}^2$ ). Due to the exquisite structure, 25 GRDs are able to be accommodated for each satellites to realize the goals of a large-sensitive area and great-localization accuracy.

The test results show that the 5.9 keV full-energy peak of the  $^{55}Fe$  source can be detected with a 70% efficiency. The readout method is simple with only one parallel channel, and the thermal noise can be suppressed by a proper discriminator threshold. This design provides a new solution for space gamma-ray detectors in the future.

## 2 The GRD Structure

The schematic diagram of the GRD is shown in Fig.1.

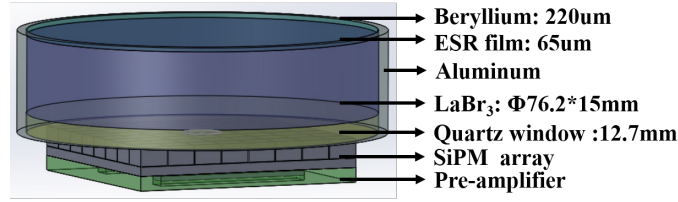


**Figure 1.** The diagram of the GRD.

The  $LaBr_3$  crystal is grown by Saint Gobain Crystal Company [10] with 76.2 mm in diameter and 15 mm-thick (Fig.2(a)), and it is sealed in an aluminum shell to avoid being deliquesced. A 220  $\mu\text{m}$  beryllium and 65  $\mu\text{m}$  ESR film are used as the incident window. The optical signals are collected by the SiPM after passing through the quartz window and then converted into electrical signals that are able to be amplified by a pre-amplifier.

The SiPMs (Version: ArrayJ-60035-64P) are produced by SensL company [11]. Each array consists of 64 independent pads with each area of  $6 \times 6 \text{ mm}^2$  to form a large  $50.44 \times 50.44 \text{ mm}^2$  sensitive area (Fig.2(b)). Biased at  $V_{br} + 6\text{V}$ , this SiPM array has a 51% photon detection efficiency (PDE) at the peak wavelength of 420 nm, and the light peak wavelength of  $LaBr_3$  is 380 nm, which is close to PDE peak.

The pre-amplifier (Fig.2(c)) is high-gain (25 times) and low wideband noise, which and the SiPM array are integrated on both sides of a PCB in order to save space and reduce the noise between the photosensor and the front-end electronics. A simple filter circuit is designed to keep the bias for the SiPM array stable. Silicone oil is filled between the quartz window and the array surface to increase light transmittance. Moreover, the area of quartz window that does not touch the array is covered by Teflon film to reduce light loss. The GRD is placed in a dark aluminum box to isolate light from outside. Due to above efforts, the 64 pads are paralleled into one channel to read optical signals.

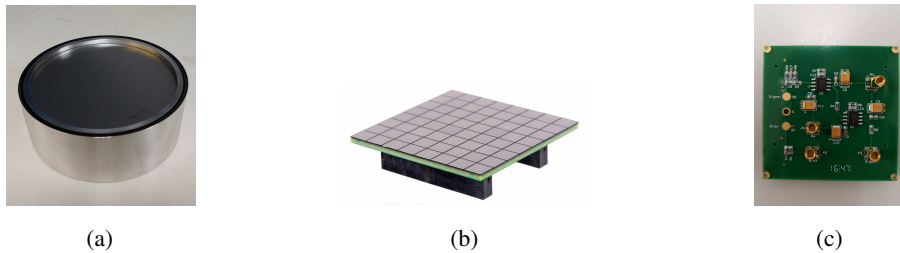


**Figure 2.** The  $LaBr_3$  crystal, the SiPM array and the pre-amplifier.

## 3 The Test System

The test system diagram (Fig.3) works at room temperature. The electrical signal is copied to two channels by CAEN N625: one enters CAEN DT5751 digitizer directly and then is recorded by the

PC, while the other is used to generate a trigger by the discriminator CAEN N840. The threshold is 7 mV, which is about twice of the baseline noise. The time window of each waveform is 3  $\mu$ s, which is much longer than the crystal's decay time because the capacitance of large area SiPM can extend the width of signals. The bias of SiPM at  $V_{br} + 4V$  to obtain a proper gain ( $> 10^6$ ). The power supply for the pre-amplifier is  $\pm 5V$  with a power consumption of 0.06 W, and the total consumption for each GRD is less than 0.1 W. Low-power consumption is a significant superiority when designing detectors for satellites.

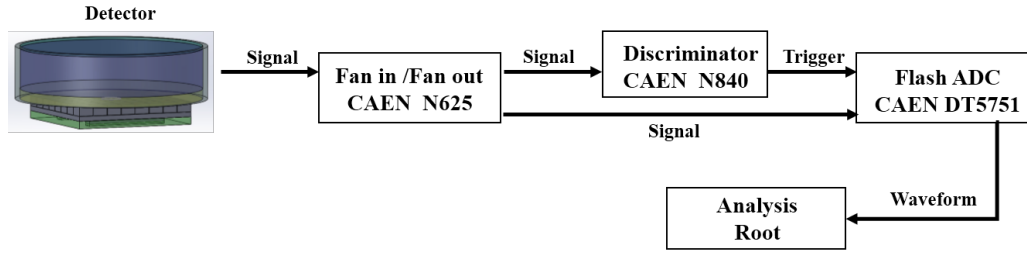


**Figure 3.** The block diagram of the test system.

A series of calibrated radioactive sources with energy ranging from 5.9 keV to 1332 keV are used to study the detectors performance. The decay of  $^{138}La$  can emit two low-energy X-rays, 5.6 keV and 37.4 keV [12]. The list of the sources with the energies of their emitted photons are listed in Table.1.

**Table 1.** The radioactive sources and activity.

Source	Energy (keV)	Branching ratio (%)	Activity (Bq)
$^{138}La$	5.6, 37.4	–	–
$^{55}Fe$	5.9	28	1270
$^{241}Am$	59.5	35.9	2.6E+05
$^{57}Co$	122, 136	85.6, 10.68	7479, 933
$^{133}Ba$	81, 356	34.06, 62.05	9.7E+04, 1.8E+05
$^{137}Cs$	662	85.1	1.1E+06
$^{60}Co$	1173, 1332	99.97, 99.98	1707, 1707

## 4 The Detector Performance

### 4.1 The low-energy performance

The 5.9 keV and the 5.6 keV X-rays are used to study the GRD low-energy performance. Fig.4 depicts the typical waveforms of effective signal and SiPM dark noise. As the red line shows, a threshold at 7 mV can distinguish the signals and the noise effectively. The energy spectra of 5.9 keV and 5.6 keV are shown in Fig.5, the full-energy peaks are obvious to be recognized. This result indicates that the GRD is sensitive to the low-energy requirement of GECAM.

The detection efficiency of a 5.9 keV X-Ray can be obtained by measuring the event rate with the  $^{55}Fe$  source (activity in Table.2). The data for 5.9 keV is 890 Hz, for which the background

event rate 280 Hz is already subtracted. Hence, the measured detection efficiency is about 70%, and the loss part is caused by the attenuation from the 220  $\mu\text{m}$  beryllium window and the 65  $\mu\text{m}$  ESR reflective film. This efficiency satisfies the target of GRD ( $> 50\%$ ).

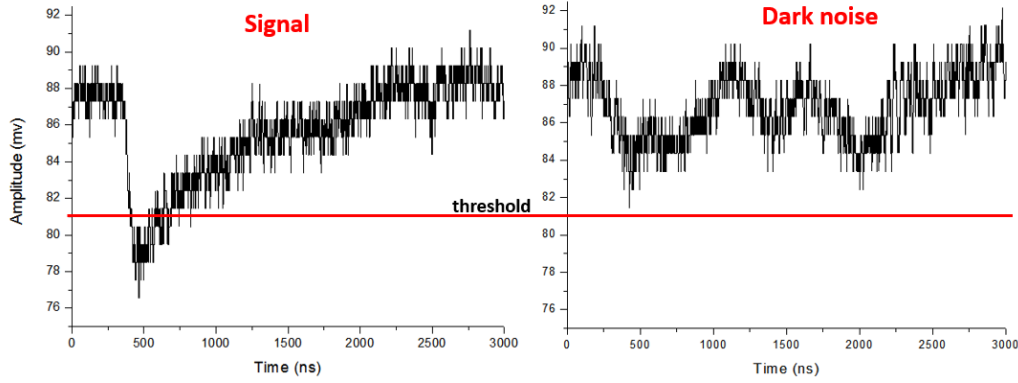


**Figure 4.** The waveforms of signal and dark noise.

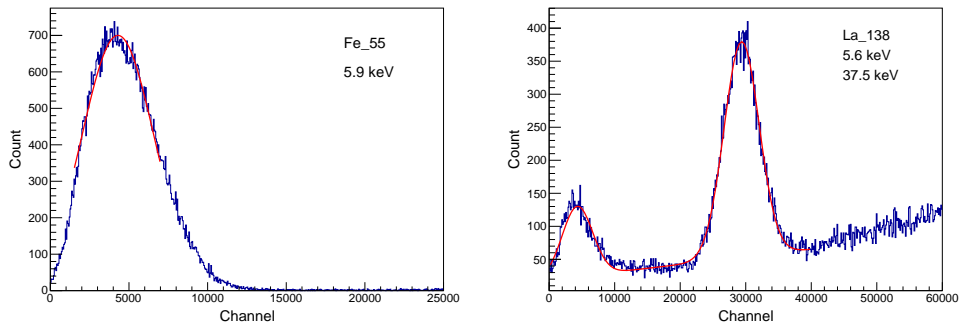


**Figure 5.** The spectra of  $^{55}\text{Fe}$  and  $^{138}\text{La}$  radioactive sources.

**Table 2.** The information of  $^{55}\text{Fe}$  source.

Source	Energy (keV)	$T_{1/2}$ (year)	$T_0$ (year)	spatial angle	Branching ratio (%)	Activity (Bq)
$^{55}\text{Fe}$	5.9	2.7	1986	$2\pi$	28	1270

## 4.2 Energy Resolution

Fig.6 shows the energy spectra of  $^{137}\text{Cs}$  and  $^{60}\text{Co}$  sources, and the energy resolution can reach 6.5% at 662 keV and 3.38% at 1332 keV. Previous studies have reported that the energy resolutions are 3% at 662 keV and 2% at 1332 keV for a small volume  $\text{LaBr}_3$  crystal coupled with a PMT [9]. Our experiment features to large area SiPM array and a large volume  $\text{LaBr}_3$  crystal to design a compact gamma-ray detector for a space telescope. The energy resolution can be influenced by several factors. The main factor is the dark noise of detector, which is 30-70 kHz/ $\text{mm}^2$  at room temperature [6], and both cross-talk and after-pulse will deteriorate the energy resolution [13].

Another factor is the uniformity, where the edge pads collect fewer scintillation photons than the center pads because the SiPM cannot cover the crystal surface completely and a part of the light might be lost. The details will be discussed in section 4.4.

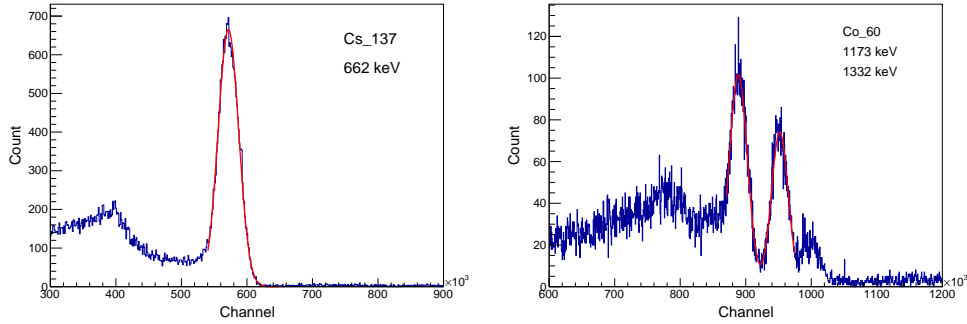


**Figure 6.** The spectra of  $^{137}\text{Cs}$  and  $^{60}\text{Co}$  and the energy resolutions are 6.5% at 662 keV and 3.38% at 1332 keV.

### 4.3 linearity

There are two elements that may influence the linearity besides the crystal quality: the response of the SiPM and the electronics. The linearity of SiPMs have a good performance according to previous experiments [13, 14]. There are 620 microcells/ $\text{mm}^2$  and more than  $10^6$  pixels for each array, so it is not saturated within the GECAM detection range. Fig.7 shows the relation between  $E_{\text{gamma}}$  and the channel number of the centroid of the peak corresponding to  $E_{\text{gamma}}$ . The linearity is preserved up to 700 keV, and then the saturation effect appears. One of the reason is that the maximum signal amplitudes that can be collected for DT5751 is only 1 V, and partial information will be lost if the  $E_{\text{gamma}}$  is higher than 700 keV, like the waveform in Fig.8. Our next work is to design a special circuit, which is able to supply a high gain for low-energy rays and a low gain for high-energy rays to record all the intact waveforms.

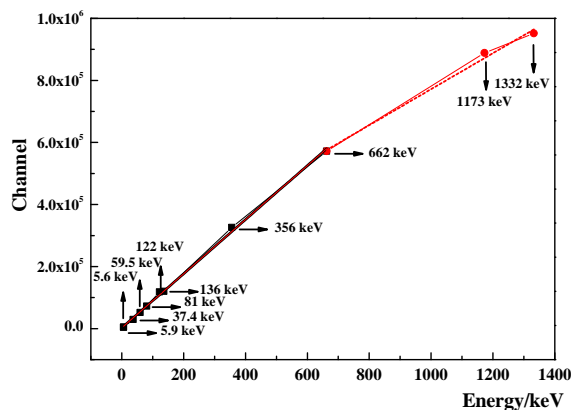


**Figure 7.** The linear relation between  $E_{\text{gamma}}$  and the channel number.

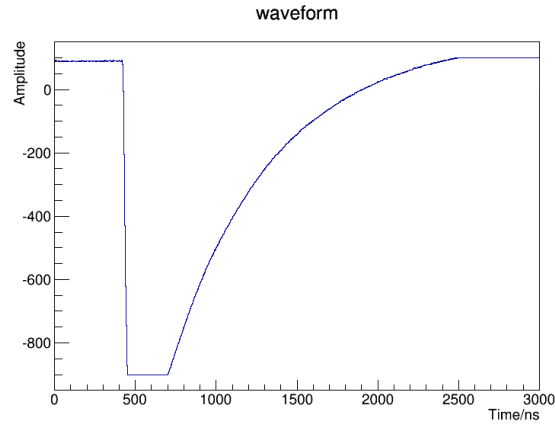


**Figure 8.** The waveforms of high-energy ray.

#### 4.4 Uniformity

The  $^{241}\text{Am}$  source is positioned 0.5 mm away from the Beryllium window surface after being collimated by 20 mm-thick lead with a hole of 3 mm in diameter, and Fig.9 shows the location over the crystal. Line 2 is at  $45^\circ$  with respect to line 1, and the distance between p1 and p2 is 10 mm (the same as p2 to p3 and p3 to p4), and p4 to p5 is 5 mm. Assuming the collected photons in the center is 1, the Y-axis shows the ratio of the other positions to the center. The area of the SiPM array is  $50.44 \times 50.44 \text{ mm}^2$ , and it cannot cover the crystal surface totally. Even though Teflon film is used to cover the exposed surface to increase reflectivity, the edge SiPM pads still collect fewer photons than center pads due to the light loss. That is the reason why the curve declines as the location moves from the center to the edge in Fig.10. Our next design is a rounded SiPM array with the same size as the  $\text{LaBr}_3$  crystal to completely cover the surface and maintain better uniformity.

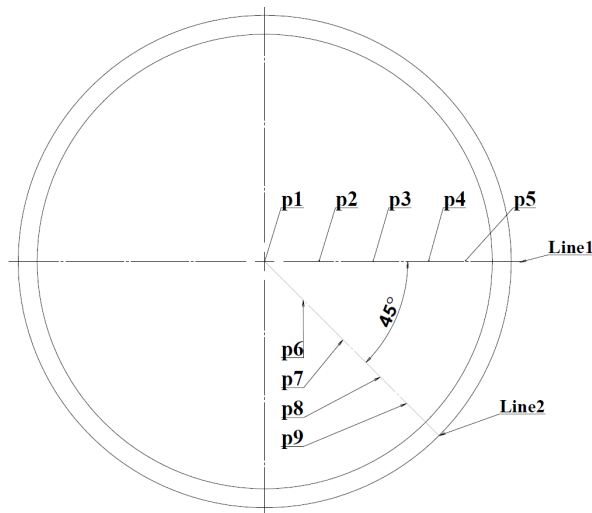


**Figure 9.** The placement of  $^{241}\text{Am}$  source above the  $\text{LaBr}_3$  crystal

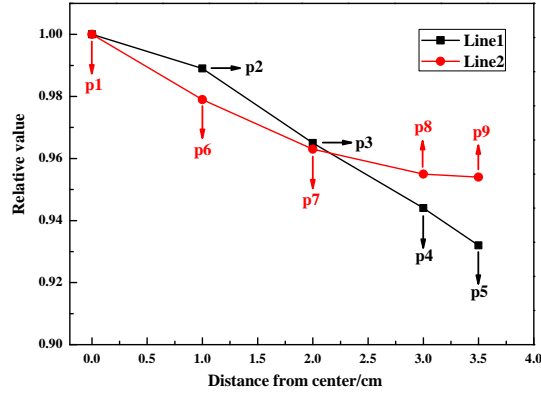


**Figure 10.** The Uniformity of the  $LaBr_3$  crystal from center to edges.

## 5 Discussion and Summary

GECAM is a dedicated space telescope that is designed for detecting high-energy electromagnetic counterpart. As its main detector, GRD must be compact, diminutive and sensitive to rays from 6 keV-2 MeV. We have reported the novel GRD performances in detail in this paper. The detector is capable of detecting the X-rays as low as 5.6 keV, which meets the GECAM requirements well. The energy resolution can reach 6.5% at 662 keV and 3.38% at 1332 keV, and the linearity is just preserved up to 700 keV due to the saturation of the digitizer. The difference in uniformity between the center and the edges is about 7%, and the X-rays detection efficiency of the entire design is 70% for 5.9 keV. The power consumption is less than 0.1W and there is only one channel electronics for each GRD.

Our next work is to optimize the GRD design and adopt a suitable circuit to enlarge the dynamic range, especially for the high-energy gamma-rays. A new rounded SiPM array is being designed, and it can solve the problem of uniformity and save space. This new kind of gamma-ray detector can be used in many areas in the future.

## Acknowledgments

The research is supported by the Key Research Program of Frontier Sciences, Chinese Academy of Sciences (Grant NO. QYZDB-SSW-SLH012).

## References

- [1] B. P. Abbott, Phys. Rev. Lett. 116 (2016) 131103.
- [2] B. P. Abbott, Phys. Rev. Lett. 116 (2016) 131102.
- [3] B. P. Abbott, Phys. Rev. Lett. 116 (2016) 061102.
- [4] B. P. Abbott, Phys. Rev. Lett. 119 (2017) 161101.



- [5] N. D'Ascenzo, JINST 10 (08) (2015) C08017.
- [6] <http://sensl.com/downloads/ds/DS-MicroJseries.pdf>.
- [7] G. Bizarri, IEEE Transactions on Nuclear Science 53 (2) (2006) 615–619.
- [8] P. Dorenbos, IEEE Transactions on Nuclear Science 51 (3) (2004) 1289–1296.
- [9] F. Quarati, Nucl Instr and Meth.A 574 (1) (2007) 115 – 120.
- [10] <http://www.detectors.saint-gobain.com/>.
- [11] <http://sensl.com/>.
- [12] F. Quarati, Nucl Instr and Meth.A 683 (2012) 46 – 52.
- [13] Y. Sun, J. Maricic, JINST 11 (01) (2016) C01078.
- [14] S. Catalanotti, JINST 10 (08) (2015) P08013.